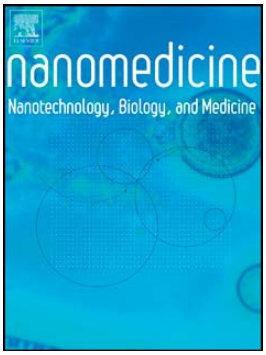

New Potential Strategies for Alzheimer's Disease Prevention: Pegylated Biodegradable Dexibuprofen Nanospheres Administration to APPswe/PS1dE9

E. Sánchez-López, M. Ettcheto, M.A. Egea, M. Espina, A.C. Calpena, J. Folch, A. Camins, M.L. García

PII: S1549-9634(16)30220-9
DOI: doi: 10.1016/j.nano.2016.12.003
Reference: NANO 1483

To appear in: *Nanomedicine: Nanotechnology, Biology, and Medicine*

Received date: 24 May 2016
Revised date: 31 October 2016
Accepted date: 6 December 2016

Please cite this article as: Sánchez-López E, Ettcheto M, Egea MA, Espina M, Calpena AC, Folch J, Camins A, García ML, New Potential Strategies for Alzheimer's Disease Prevention: Pegylated Biodegradable Dexibuprofen Nanospheres Administration to APPswe/PS1dE9, *Nanomedicine: Nanotechnology, Biology, and Medicine* (2016), doi: 10.1016/j.nano.2016.12.003

NEW POTENTIAL STRATEGIES FOR ALZHEIMER'S DISEASE PREVENTION: PEGYLATED BIODEGRADABLE DEXIBUPROFEN NANOSPHERES ADMINISTRATION TO APPswe/PS1dE9

Sánchez-López E.[a,b], Ettcheto M.[c,d], Egea M.A.[a,b], Espina M.[a,b], Calpena A. C. [a,b], Folch, J [d,e], Camins A.[c,d], García M. L.[a,b*]

[a] Department of Pharmacy, Pharmaceutical Technology and Physical Chemistry, Faculty of Pharmacy, University of Barcelona.

[b] Institute of Nanoscience and Nanotechnology (IN2UB), Faculty of Pharmacy, University of Barcelona.

[c] Department of Pharmacology and Therapeutic Chemistry, Faculty of Pharmacy, University of Barcelona.

[d] Biomedical Research Networking Center in Neurodegenerative Diseases (CIBERNED), Madrid, Spain

[e] Biochemistry unit, Faculty of Medicine and Health Sciences, University Rovira i Virgili, Reus (Tarragona), Spain.

*__Corresponding autor__: Maria Luisa García López. Department of Pharmacy, Pharmaceutical Technology and Physical Chemistry, Faculty of Pharmacy, University of Barcelona, 08028, Barcelona, Spain. Phone: +34 93 402 45 52. Fax: +34 934 035 987. marisagarcia@ub.edu

Word count for the Abstract: 145

Word count for the Manuscript (body text and figure legends): 4751 + 248 = 4999

Number of Figures: 7

Number of references: 52

Number of Tables: 1

Number of Supplementary Material files: 1

Abstract

Dexibuprofen loaded pegylated poly(lactic-co-glycolic) nanospheres prepared by solvent diffusion method were designed to increase Dexibuprofen brain delivery reducing systemic side effects. Nanospheres exhibited a mean particle size around 200 nm (195.4 nm), monomodal population and negative surface charge. Drug loaded nanospheres showed a sustained release profile, allowing to modify the posology *in vivo*. Nanospheres were non-toxic neither in brain endothelial cells nor astrocytes and do not cause blood-brain barrier disruption. Nanospheres were able to partially cross the cells barrier and release the drug after co-culture *in vitro* experiments, increasing Dexibuprofen permeation coefficient. Behavioral tests performed in APPswe/PS1dE9 mice (mice model of familial Alzheimer's) showed that nanospheres reduce memory impairment more efficiently than the free drug. Developed nanospheres decrease brain inflammation leading to β-amyloid plaques reduction. According to these results, chronical oral Dexibuprofen pegylated poly(lactic-co-glycolic) nanosystems could constitute a suitable strategy for the prevention of neurodegeneration.

Keywords: nanoparticles, nanospheres, PLGA-PEG, Dexibuprofen, blood-brain barrier, Alzheimer's disease.

Abbreviations: Alzheimer's disease, AD; β-amyloid, Aβ; non-steroidal anti-inflammatory drugs, NSAIDs; Dexibuprofen, DXI; poly(lactic-co-glycolic acid), PLGA; Food and Drug administration, FDA; nanoparticles, NPs; poly(ethylene glycol), PEG; nanospheres, NSs; polyvinyl alcohol (PVA); Mean average size, Z_{av}; polydispersity index, PI; zeta potential, ZP; encapsulation efficiency, EE; transmission electron microscopy, TEM; Akaike's information criterion, AIC; endothelial permeation coefficient, P_e; phospo-cAMP response element-binding, p-CREB; human serum albumin, HSA; Activity-Regulated Cytoskeleton-associated, ARC; brain-derived neurotrophic factor, BDNF

Background

Currently, Alzheimer's disease (AD) is a multifactorial and incurable neurodegenerative condition highly prevalent in old age. [1] It is widely accepted that brain increase in β-amyloid (Aβ) levels, mainly Aβ42, and TAU phosphorylation are the main markers of the disease. Thus, approximately 25 years ago Hardy et al.[2] proposed the "amyloid cascade hypothesis", where Aβ42 was primarily responsible of neuronal damage in AD. However, it has been demonstrated that Aβ42 cannot completely explain the process of neuronal loss in AD because drugs developed against βA42 do not improve all the related disease symptomatology. Thus, alternative hypothesis had been developed, among them, the neuroinflammatory hypothesis where AD could be considered as a chronic brain inflammatory process. Neuroinflammatory responses are characteristic of pathologically affected tissue in neurodegenerative disorders such as Parkinson disease, epilepsy and AD. [3] Several evidence has been found indicating that increased peripheral inflammation leads to more neurodegeneration and accelerated disease progression in animal models. [4]

Inflammation occurs in vulnerable regions of the AD brain, with increased expression of acute phase proteins and proinflammatory cytokines, which are hardly evident in a normal brain. Glial cells (microglia and astrocytes) are responsible for the inflammatory reaction through the generation of inflammatory mediators stimulated by βA42 oligomers and plaques containing dystrophic neurites. Chronically activated glial cells can contribute to neuronal dysfunction and cell death through the release of highly toxic products.[5]

Several studies confirm that the long-term treatment with non-steroidal anti-inflammatory drugs (NSAIDs) such as ibuprofen, reduce the risk of AD, delay disease onset, ameliorate symptomatic severity, and slow cognitive decline. [3, 6] However, an important clinical limitation of ibuprofen, and in general of NSAIDs clinical administration, are the gastrointestinal adverse effects. These can be reduced by the use of the active enantiomer, dexibuprofen (DXI), which is twice more potent than the former. [7] DXI has been assessed on short-term treatment by Jin and co-workers[3] on animal models of AD achieving successful results. In clinical studies, this enantiomer demonstrates to cause less side effects than the racemic mixture being therefore a good candidate to prevent AD. However, the typical secondary effects associated with NSAIDs (such as gastric toxicity) still appeared in human trials and would increase with long-term ad-

ministration. [7, 8, 9] In addition, due to the low water solubility of DXI, this drug exhibits many *in vivo* limitations like incomplete release, poor bioavailability, food interactions, and high inter-subject variability. [10] Side effects caused by continuous DXI administration could be overcome by the use of the drug encapsulated on nanostructured systems. To carry the drug across the blood-brain-barrier (BBB), facilitate its posology and avoid undesired side effects, polymeric nanoparticles (NPs) have been proposed.

Biodegradable polymers such as poly(lactic-co-glycolic acid) (PLGA) had been approved by the Food and Drug administration (FDA) and used as colloidal carriers for drug controlled release. [11, 12] Among other carriers, PLGA possess several advantages such as its biocompatibility, biodegradability and non-toxicity. Furthermore, these synthetic polymers demonstrate higher reproducibility, are easily formulated and allow the control and prediction of the degradation kinetics. [13] Coating of PLGA NPs with poly(ethylene glycol) (PEG) represents an improvement since it increase particles circulation avoiding their recognition by the reticuloendothelial system. [14]

The main goal of this work was the development of a formulation for brain delivery of DXI, based on nanospheres (NSs) composed of PLGA surrounded by PEG chains (DXI- PLGA-PEG NSs). The suitability of DXI-PLGA-PEG NSs to treat and prevent inflammation associated with AD has been demonstrated. *In vitro* studies of NSs transport across the BBB were undertaken and *in vivo* effectivity of the developed NSs on transgenic mice for AD were carried out.

Methods

PLGA-PEG 5% Resomer® was obtained from Evonik Corporation (Birmingham, USA) and the active compound *S*-(+)-Ibuprofen (dexibuprofen) was purchased from Amadis Chemical (Hangzou, China). Water filtered through Millipore MilliQ system was used for all the experiments and all the other reagents were of analytical grade.

Nanospheres production

NSs were prepared by solvent displacement method described elsewhere. [15] NSs mean size (Z_{av}) and polidispersity index (PI) of DXI loaded PLGA-PEG NSs were determined by photon correlation spectroscopy (PCS) using a ZetaSizer Nano ZS (Malvern Instruments). Measurements were carried out by triplicate at angles of 180^{o} in 10 mm diameter cells at 25 ^{o}C. Zeta potential (ZP) was calculated from electrophoretic mobility. [16]

The encapsulation efficiency (EE) of DXI in the NSs was determined indirectly. The non-entrapped DXI was separated using filtration/centrifugation. DXI was measured by HPLC method as is described on previous publications. [17]

Design of experiments

Design of experiments (DoE) was applied to optimize formulation parameters using a full factorial design. [18] Series of independent parameters and their influences in DXI loaded NSs were studied, determining the effects and interactions between factors. [19]

As can be observed on Table 1, concentration of each formulation compound and pH of the aqueous phase were used as independent variables and Z_{av}, PI and ZP of the NSs were studied.

Nanospheres characterization

To visualize the optimized DXI loaded NSs, negative staining was carried out with uranyl acetate (2%) on copper grids activated with UV light. NSs morphology was determined by transmission electron microscopy (TEM), performed on a JEOL 1010 microscope (Akishima, Japan).

Storage stability

DXI loaded NSs stability at 4, 25 and 38 ^{o}C was assessed studying light backscattering and transmission profiles by using Turbiscan®Lab. For this purpose, a glass measurement cell was filled with 20 ml of sample. The radiation source was a pulsed near infrared light and was received by a transmission and backscattering detectors at an

angles of 90 and 45° from the incident beam, respectively. Data were acquired once a month for 24 h at 1 h intervals.

In vitro drug release

An inverse dialysis was performed under "sink conditions". This technique is based on the dispersion of the colloidal suspension in the dialysis medium (buffer solution) at 37°C. [20] At predetermined intervals, one sac containing 1 ml of sample was withdrawn from the stirred release medium and simultaneously replaced with 1 ml of fresh buffer at the same temperature.

Akaike's information criterion, AIC, was determined as an indicator of the model's suitability for a given dataset. The model associated to the smallest AIC value is considered as giving the best fit of the set of data. [19]

Cell culture

Different cell lines were cultured for *in vitro* studies: cells derived from rat pheochromocytoma (PC12), mouse microvascular endothelial cells (bEnd.3 cells) and primary glial cells from brain rat cortex (astrocytes). PC12 cells were obtained from Sigma-Aldrich®. Primary cultures of astrocytes were obtained from bank Gaiker-IK4 culture. Glial cells were from Sprague Dawley cerebral cortex of newborn rats. The endothelial cell line was maintained in its specific culture medium. [21]

Cytotoxicity studies

The dye Alamar Blue is widely used as indicator of cell viability. [22] Absorbance was determined at λ of 570 nm (reduced form) and 620 nm (oxidized form) after incubating the cells with DXI NSs at different concentrations for 24 h. Data were analyzed by calculating the percentage of Alamar blue reduction and expressed as percentage of control. [22, 23]

In vitro transport across the BBB

In vitro BBB models have become a standard tool to estimate the ability of drugs to overcome this barrier. [24] For co-culture experiments, bEnd.3 cells were seeded in the apical part of polycarbonate transwell inserts. A semipermeable filter was placed and in the basolateral compartment cells from primary cultures of rat astrocytes were added at a density of $6 \cdot 10^4$ cells/ml. [25]

Trans-epithelial electrical resistance (TEER) manual measurements were taken daily until a steady state was reached. To calculate the TEER of each insert, the equation /1/ was applied and values are expressed in $\Omega \cdot cm^2$.

$$TEER = [\Omega \text{ cell monolayer} - \Omega \text{ filter (without cells)}] \cdot \text{filter surface} \qquad /1/$$

bEnd.3 cells were co-cultured on the apical part of the inserts placing astrocytes on the basolateral compartment. Inserts were removed and placed in new media plates with Hanks + 0.5% bovine serum albumin (BSA). Apical media was removed, washed with Hanks and DXI loaded NSs were added in the apical part of the inserts and were left for one hour.

In order to verify that DXI loaded NSs do not cause membrane disruption, a low paracellular permeability compound was added and quantified at the end of the study, namely, Lucifer yellow (LY). Membrane integrity was determined.

NSs quantification on the basolateral compartment was carried out measuring PEG chains on a Triple Quadrupole LC/MS/MS Mass Spectrometer in MRM with a positive mode. Source was a Turbo Spray a 400 ^oC and separation module was a UPLC Acquity. Mobile phase was composed of methanol: water (0.1 % formic acid) and a gradient was applied. Mass variation was recorded at 710.8 and 89.10 Da. Proton nuclear magnetic resonance spectra (^{1}H-NMR) was used to confirm that PLGA-PEG DXI structure after crossing the barrier. The spectrum was recorded at 298 K on a Varian Inova 500 MHz spectrometer (Agilent Technologies, Santa Clara, CA, USA) [26].

Cellular uptake

Cellular internalization was measured by labelling the DXI NSs with Rhodamine. PC12 cells were cultured, collected, counted and then transferred to a 24-well plate and incubated overnight. Then the cell culture medium was replaced with medium containing Rho DXI NSs (2.5 mg/ml) and incubated for a predetermined times (5, 10,

15 and 30 min). After incubation, suspended NSs were removed and cells were washed trice with PBS to remove unbound NSs. Cell membranes were permeabilized by cell lysis solution and the fluorescence was read by spectrofluorometric methods. [27]

In vivo studies

Male APPswe/PS1dE9 (APP) and C57BL/6 mice age matched with the same background were used. APP/PS1 animals co-express a Swedish (K594M/N595L) mutation of a chimeric mouse/human APP (Mo/HuAPP695swe), together with the human exon-9-deleted variant of PS1 (PS1-dE9), allowing these mice to secrete elevated amounts of human Aβ peptide. [28] The animals were kept under controlled temperature, humidity and light conditions with food and water provided *ad libitum*. Mice were treated in accordance with the European Community Council Directive 86/609/EEC and the procedures established by the Department d'Agricultura, Ramaderia i Pesca of the Generalitat de Catalunya. Every effort was made to minimize animal suffering and to reduce the number of animals used. Forty 6 month-old animals, divided into four groups were used for the present study.

Biodistribution studies

Biodistribution was determined with Rho DXI NSs and 300 µl were administered by oral gavage. After 24 h, animals were sacrificed and tissues were weighted, collected, and homogenized. DXI NSs extraction with methanol was carried out and fluorescence of Rhodamine was measured by fluorescence spectrometry at λ_{ex} 553nm and λ_{em} 627 nm. Data was normalized with the negative control from mice treated with saline only.

Long-term treatment *in vivo* studies

Mice were treated for three months with DXI at therapeutic doses (50 mg/kg/day) and DXI loaded NSs were administered on alternate days. [28, 29] NSs volume was calculated for each animal previously weighted and was administered on a drinking bottle. Afterwards, NSs drinking bottle was replaced by untreated water for 24 hours.

Following *in vivo* testing, the animals were sacrificed and at least 6 mice in each group were used for histological studies. [30]

Gastric damage

After treatment, mice were sacrificed and stomachs were removed, cut and rinsed with ice-cold distilled water. The ulcer index (UI) was determined.[31, 32] The severity of the lesions was calculated as reported by other authors. [33] After scoring, the stomachs were frozen at -20 ºC for 24 h. Samples were allowed to thaw at room temperature losing the surface mucosa from the underlying tissue. The mucosa was removed by scrapping with the edge of a microscope slide, freeze dried and weighted.[32]

Morris water Maze

The Morris water maze (MWM) test was conducted in a circular tank. The water tank was colored white at a temperature of 21 ± 2 °C. A white platform was submerged in the middle of the northeast quadrant. Behavioral data were acquired and analyzed using a computerized video tracking system. The test procedure consisted of a six-day navigation testing with five trials per day and a probe trail. Animals were allowed to swim freely for 60 s to seek the platform and allowed to remain there for 10 s. If after 60 s a mouse was not able to find the platform, it was guided to it and left there for 30 s. The probe trail was performed the day after the last training test. This day, the hidden platform was removed, and the mice were released from the southwest quadrant and allowed to swim for 60 s. Results were calculated individually for each animal. [34]

Western blot analysis

Aliquots of hippocampus homogenate were analyzed using the Western blot method and normalized to GAPDH as previously described [35] Measurements are expressed as arbitrary units.

Immunohistochemistry studies

To elucidate whether the differences in the cognitive behavior correlate with AD-related pathology on the brain, mice were anesthetized with sodium pentobarbital and perfused with 4 % paraformaldehyde. Brains were stored at 4 ^{o}C overnight dehydrated in 30 % phosphate-buffered sucrose solution. Samples were preserved at -80 ^{o}C and coronal sections of 20 µm were obtained by a cryostat (Leica Microsystems, Wetzlar, Germany).

Sections were incubated overnight at 4 °C with the rabbit antibodies against GFAP (1:2,000; Dako, Glostrup, Denmark) and IBA-1 (1:1000, Wako) and sequentially incubated for 2 h with Alexa Fluor 594 goat anti-rabbit antibody at room temperature (1:500; Invitrogen, Eugene, OR, USA). Images were processed using ImageJ by comparing the different conditions and quantifying the integrated density.

Staining of β-Amyloid plaques was performed using Thioflavin S (ThS 0.002 %, Sigma-Aldrich). Sections were counterstained with 0.1 µg/ml Hoechst 33258 (Sigma-Aldrich, St Louis, MO, USA). [36] Samples were additionally stained with monoclonal anti-βA 1-42 (1:1000; Covance, USA) at 4ºC overnight. [37]

Samples were visualized using a fluorescence microscope (BX41 Laboratory Microscope, Melville, NY-Olympus America Inc). For each image, the proportion of total image area covered by fluorescently stained β-amyloid plaques was quantified. For each mouse, four fields per section with the highest density of plaques were chosen as representative and averaged. [38]

Statistical analysis

All of the data are presented as the mean ± S.D. Two-way ANOVA followed by Tukey post hoc test was performed for multi-group comparison. Student's *t*-test was used for two-group comparisons. Statistical significance was set at $p < 0.05$ by using GraphPad 5.00 Prism.

Results

Design of experiments

Design of experiments (DoE) was used to optimize formulation parameters in order to obtain small and monomodal DXI loaded NSs (Z_{av} < 200 nm, PI < 0.1) able to cross the BBB. Regarding NSs size, polymer concentration and PVA amount are the factors presenting a significant relationship ($p<0.05$). As is shown in Figure 1A, increasing both polymer and surfactant concentration leads to higher NSs Z_{av}. The opposite effect was found regarding PI, were high polymer concentrations produced to less NSs size dispersion. As can be observed in Table 1, ZP values are negative due to polymer negative charge. Subsequently, higher polymer concentrations lead to more negative surface charge being NSs more stable ($p<0.05$). [17] As is shown in Figure 1B, this parameter is also affected by DXI concentration in an inverse relationship probably due to DXI masking of NSs surface charge. EE results show that as DXI amount increased, EE was also higher. This could be probably due to the great polymer entrapment capacity which is not reached at the studied concentrations and also to the PEG chains in which the drug remains adsorbed. The maximum EE was obtained when the pH of the aqueous phase was similar as the pK_a of the drug (DXI pK_a 4.65). However, this pH increases NSs PI (Figure 1C).

With this trends, a formulation was optimized. Optimized DXI loaded NSs formulation contain 4.5 mg/ml of DXI, 7 mg/ml of polymer, a low PVA amount (10.0 mg/ml) and a pH of 3.8. NSs were centrifuged at 15000 r.p.m. for 30 minutes and observed by TEM (Figure 2) showing a round shape and a smooth surface.

In vitro release

DXI release data from the NSs was adjusted to hyperbola equation. Initial release corresponds to a burst effect, probably due to the drug adsorbed on NSs surface due to PEG chains. [39] DXI release from the NSs at 6 h achieves a maximum plateau (B_{max}) at 66.65 ± 1.27 %, lower than free DXI. Dissociation constant (K_d), for DXI loaded NSs, which corresponds to the time where 50 % of the drug is released, was 46.8 ± 3.0 minutes. These results suggest a faster release as more drug is encapsulated inside the NSs.[17] This would probably be due to the fact that after 6 hours, the NSs are still

achieving a sustained drug release whereas after 2 hours free DXI was completely released.

Storage stability

Storage stability assays at different temperatures showed that DXI loaded NSs were stable for two months at 25 and at 4 ^{o}C. In Figure 3A and 3B, backscattering and transmission profiles at each temperature could be observed. it could be noticed that samples are unstable within two months (differences of backscattering above 10%). [40] As was shown on previous publications, samples present high levels of instability at 38 ^{o}C at the end of the first month (Figure 3C) due to polymer degradation processes. [17] These results are in agreement with those obtained by other authors for these polymeric nanostructured systems. [19]

Cytotoxicity assays

Cell viability was studied in both astrocytes and bEnd.3 cells prior to *in vitro* transport experiments. In addition, cytotoxicity was assessed in PC12 cell line.[41, 42] As is shown in Figure 4A, in all the cell lines assessed, cell viability was higher than 80%, thus meaning that DXI loaded NSs do not damage neither endothelial brain cells nor neuronal cells in any of the assessed concentrations. These results suggest that the develop would be biocompatible with brain cells.[43]

***In vitro* BBB transport**

Co-culture systems effectivity to predict the transport of drugs across the BBB has been demonstrated by other authors. [24] Graphical evidence of the NSs on the basolateral compartment after 1 hour of incubation could be observed in Figure 4B. In addition, H^1-NMR results show that both NSs peaks and DXI were present on the basolateral media (supplementary material S1).

According to LY used as a control, NSs at 2.5 mg/ml do not cause damage on the cells forming the BBB being able to preserve membrane integrity. 31.4 % of the initial NSs remain inside the cells barrier. DXI was quantified on the basolateral and apical

compartments, 28% of the drug was retained by the cells within one hour and drug endothelial permeability coefficient, P_e, was 0.99 cm/s.

Cellular uptake

In order to elucidate if the developed NSs would be able to be internalized by the cells, NSs were labelled fluorescent with Rhodamine (Rho). Fluorescence was measured after cell lysis at different times for both Rhodamine and DXI as is shown in Figure 4C. DXI NSs were found to penetrate almost 100 % after the first 5 minutes of incubation and therefore, DXI would be released inside the cells. In addition, a decreasing in free Rho uptake confirm that the cellular uptake was not due to the additional fluorescent coating.

Biodistribution studies

24 hours after Rho DXI NSs administration by oral gavage, a considerable amount of NSs remain on the liver (supplementary material, S2). However, developed NSs were found also on the brain (0.37 mg/ml NSs /g tissue). PEGylation of PLGA NPs post-oral administration demonstrated to increase transport across the BBB. [44] PEGylated NPs have been reported to promote mucus penetration and increase drug half-life, in this case, after 24 hours, NSs remain in the brain. [45] Despite this fact, accumulation can be observed on the liver probably due to the elimination route of the nanosystems via uptake of Kupffer cells.

Morris water maze and western blot analysis

The effect of DXI loaded NSs and free DXI on the spatial learning and memory deficits in APP mice were conducted using the Morris water maze test.

Escape latency of all groups trough the training days is supplied as supplementary material (S3). A clear trend could be stablished towards mice learning where untreated and free DXI treated groups showed similar learning capacities whereas DXI loaded NSs group present an evolution more similar to WT groups. In Figure 5 results corresponding to the probe trail could be observed. In Figure 5A, statistically significant differences were obtained regarding escape latency between transgenic groups treated either with free DXI or DXI loaded NSs compared with untreated APP animals. In addition, escape latency media corresponding to DXI loaded NSs was lower than the obtained for the free drug.

Regarding the time % in platform zone (Figure 5B), DXI loaded NSs spend higher percentages on this area whereas transgenic control group show no tendency to find the platform. Significant differences were obtained compared with the untreated groups with DXI loaded NSs, whereas free DXI do not shown significant values. The number of times that the animals cross the platform zone is supplied as supplementary material S4. In this parameter, also significant differences are observed with DXI loaded NSs and untreated transgenic groups. The same tendency but without statistical differences were observed for the number of entries on the platform (Supplementary material S5). Interestingly, our western-blot results, showed in Figure 5C and 5D, demonstrated that DXI increase the levels of monophosphate response element-binding protein (p-CREB).

Gastric damage

As can be observed on Figure 6A, DXI NSs did not shown significant differences on gastric damage compared with control group. Free drug produced an increase on stomach lesions compared with DXI NSs and control group. Similar results were obtained measuring the mucosal weight showing that free DXI produce significant differences against control group ($p<0.05$) as can be observed on Figure 6B.[32]

Immunohistochemistry studies

The formation of Aβ plaques, which is a pathologic hallmark of AD, could be observed by Thioflavin-S staining. Figure 6A shows results corresponding to amyloid plaques counting of APP/PS1 mice on brain cortex. ThS staining was negative for WT groups indicating the absence of fibrillar Aβ. [46] APP mice treated with DXI loaded NSs developed a certain number of plaques, which levels were significantly lower than those obtained for the rest of transgenic groups ($p<0.001$), including free DXI groups. In addition, as can be observed in Figure 6B, plaques developed by free DXI or DXI loaded NSs groups were smaller than the untreated APP group.

Glial cells are the source of released cytokines, which are implicated in the formation of Aβ plaques on AD development. [47] GFAP reactive cells had been defined as an indicator for astrocyte activation and, as is shown in Figure 7A and 7C, the number of reactive cells on the hippocampal brain sections of animals treated by DXI loaded NSs was lower than the untreated transgenic group. The same results, presented on Figure 7B and 7D, were obtained regarding microglial activation (IBA1) showing DXI NSs

significant differences ($p<0.05$) with the untreated transgenic groups. In addition, non-significant differences were obtained between DXI loaded NSs and DXI administered continuously.

Discussion

Current therapeutic strategies for AD, suggest that modulation or prevention of chronic neuroinflammation process could be a suitable target for AD prevention. In the present manuscript, we have demonstrated in APP/PS1 mice that DXI loaded NSs have a beneficial effect on key markers of AD namely Aβ plaque formation, glial activation and memory impairment.

The BBB is one of the most restrictive barriers of the body allowing only small molecules such as the developed NSs to cross it. With the purpose to achieve brain drug release upon oral administration, DoE was applied to establish useful trends in NSs behavior in order to obtain a suitable formulation. To obtain NSs Z_{av} below 200 nm with high EE, an intermediate PLGA-PEG concentration and a high drug amount were chosen. The optimized NSs showed EE > 99 %, Z_{av} < 200 nm and a narrow monomodal population. The *in vitro* prolonged release of DXI from the NSs could contribute towards a decrease of drug the drug regime dosage and reduced side effects such as gastric toxicity, both improving patient adherence to the treatment.

Cytotoxicity studies confirm that the developed formulation does not affect cell viability neither on the cells of the BBB (bEnd.3 and astrocytes) or in neuronal cells (PC12). *In vitro* transport across the BBB experiments, show both DXI loaded NSs safety towards the BBB structure without compromising barrier's limited permeability and also suggest that the DXI NSs produced a prolonged release. These results, along with the *in vitro* drug release suggest that NSs would release the drug slowly and part of the NSs would cross the BBB during the first hours of administration, as is confirmed by H^1-RMN and TEM. Ibuprofen is reported by other authors [48] to be poorly distributed to the brain with P_{app} values oscillating between 0.31 and 0.41 To overcome this, optimized NSs would increase free drug P_e proving to be beneficial for brain delivery regarding free drug formulation. [48, 49] This could be due to the flexibility of PEG chains which act as a protective shield on the particles surface giving them the so-called stealth properties. [50]

According to other authors, PEGylated PLGA NSs would enter later into the cells by claritin-mediated endocytosis. [50]

Biodistribution assays demonstrate that NPs are able to cross the BBB and remain in the brain 24 h after administration. Due to the higher surface area of the NPs and the increased mucoadhesitvity is probable that they are captured by the mucous layer of the GI tract and they are endocited and arrive to the brain via systemic circulation. High concentrations founded in the liver demonstrate that the elimination route would be via hepatic circulation. In addition, DXI NSs decrease gastric damage produced by the free drug.

In vivo experiments carried out comparing transgenic mice either without treatment or treated with the free drug or with DXI loaded NSs administered on alternate days showed that DXI NSs were more effective on spatial memory improvement than free DXI or untreated animals. In short, these results demonstrated that DXI loaded NSs could improve memory impairment compared to both free DXI and untreated transgenic groups. These positive results of DXI NSs against the free drug can be attributed to drug encapsulation and prolonged release into PEGylated NSs since PEGylation contributes to increase transport across the BBB.[50, 51]

In brain cortex, DXI loaded NSs induce a significant amylogenesis decrease, which is one of the hallmarks of AD. Although the mechanism by which inflammation reduction inhibits amylogenesis have not been completely elucidated, a clear relationship is well known between Aβ plaques development and both astrocytes and microglial activation. [47] In the central nervous system, astrocytes and microglial cells are the main types of cells in the inflammatory response. [4] In a non-activated state (physiological conditions) glial cells are of great importance for neuronal plasticity processes and Aβ clearance and degradation. However, under certain conditions related to chronic stress, the role of glial cells may not be beneficial. Effectively, activation of glial cells induce morphologic changes, releasing cytokines, and neurotoxic agents that can worsen CNS damage. [5] Interestingly, we demonstrated that brain glial activation in APP mice is prevented effectively by DXI loaded NSs administered on alternate days. These results are in agreement with those obtained for microglial inflammation reduction. Since Aβ42 oligomers and their precursor APP are potent glial activators, our data reinforce the potential chronic application of DXI loaded NSs in AD prevention. Obtained data indicates that DXI loaded NSs, prevent amylogenesis induced by neuroinflammatory processes by blocking cytokines release and glial activation. [47] These results are in

accordance with behavioral assays, indicating that DXI restored cognition by inhibiting the neuroinflammatory response associated with AD thus decreasing insoluble amyloid plaques and interestingly at the molecular levels through the increase of p-CREB. This data is relevant because an increase in p-CREB levels leads to the transcription of memory-associated genes such as *c-fos, ARC, BDNF* that are involved in the process of learning and memory. [52]

In summary, the current study shows that treatment with DXI loaded NSs represent an improvement for AD neuropathological markers, mainly a significant reduction of brain Aβ accumulation, glial activation and improved cognitive performance in APP mice. In addition, DXI loaded NSs were safe for brain cells and suitable for oral administration. Pegylated NSs were capable of increasing drug permeability across the BBB without cause disruption of the BBB. Thus, we suggest that DXI loaded NSs could be a suitable and safe strategy for a chronic treatment for AD prevention.

Acknowledgments

This work was supported by the Spanish Ministry of Science and Innovation (MAT2014-59134-R projects). The first author ESL acknowledges the support of the Spanish Ministry for the PhD scholarship FPI-MICINN under the reference BES-2012-056083. MLG, ACC, ME, MAE and ESL belong to 2014SGR-1023 and AC and ME belong to 2014SGR 525.

References

1. Folch, J. *et al.* Current Research Therapeutic Strategies for Alzheimer' s Disease Treatment. *Neural Plast.* **2016,** 1–15 (2016).
2. Hardy, J. A. & Higgins, A. Alzheimer's disease: the amyloid cascade hypothesis. *Perspective* **256,** 184–185 (1992).
3. Jin, D.-Q. *et al.* Dexibuprofen (S(+)-isomer ibuprofen) reduces microglial activation and impairments of spatial working memory induced by chronic lipopolysaccharide infusion. *Pharmacol. Biochem. Behav.* **89,** 404–411 (2008).
4. Wyss-coray, T. & Rogers, J. Inflammation in Alzheimer Disease — A Brief Review of the Basic Science and Clinical Literature. *Cold Spring Harb. Perspect. Biol.* 1–24 (2012). doi:10.1101/cshperspect.a006346
5. Rubio-Perez, J. M. & Morillas-Ruiz, J. M. A Review: Inflammatory Process in Alzheimer's Disease, Role of Cytokines. *Sci. World J.* **2012,** 1–15 (2012).
6. Tabet, N. & Feldmand, H. Ibuprofen for Alzheimer's disease. *Cochrane Database Syst* **Rev 2,** (2003).
7. Kaehler, S. T., Phleps, W. & Hesse, E. Dexibuprofen: pharmacology, therapeutic uses and safety. *Inflammopharmacology* **11,** 371–383 (2003).
8. Bonabello, A. *et al.* Dexibuprofen (S(+)-Isomer Ibuprofen) reduces gastric damage and improves analgesic and antiinflammatory effects in rodents. *Anesth. Pharmacol.* **97,** 402–408 (2003).
9. Phleps, W. Overview on clinical data of dexibuprofen. *Clin. Rheumatol.* **20,** S15–21 (2001).
10. El-Houssieny, B. M., El-Dein, E. Z. & El-Messiry, H. M. Enhancement of solubility of dexibuprofen applying mixed hydrotropic solubilization technique. *Drug Discov. Ther.* **8,** 178–184 (2014).
11. Salem, S. A. *et al.* Polylactic-co-glycolic acid mesh coated with fibrin or collagen and biological adhesive substance as a prefabricated, degradable, biocompatible, and functional scaffold for regeneration of the urinary bladder wall. *J. Biomed. Mater. Res. - Part A* **101 A,** 2237–2247 (2013).
12. Graf, N. *et al.* αvβ3 Integrin-targeted PLGA-PEG nanoparticles for enhanced anti-tumor efficacy of a Pt(IV) prodrug. *ACS Nano* **6,** 4530–4539 (2012).

13. Anderson, J. M. & Shive, M. S. Biodegradation and biocompatibility of PLA and PLGA microspheres. *Adv. Drug Deliv. Rev.* **64,** 72–82 (2012).

14. Griffiths, P. C., Cattoz, B., Ibrahim, M. S. & Anuonye, J. C. Probing the interaction of nanoparticles with mucin for drug delivery applications using dynamic light scattering. *Eur. J. Pharm. Biopharm.* **97,** 218–222 (2015).

15. Vega, E. *et al.* PLGA nanospheres for the ocular delivery of flurbiprofen: drug release and interactions. **97,** 5306–5317 (2008).

16. Vega, E. *et al.* Flurbiprofen PLGA-PEG nanospheres: role of hydroxy-β-cyclodextrin on ex vivo human skin permeation and in vivo topical anti-inflammatory efficacy. *Colloids Surfaces B Biointerfaces* **110,** 339–346 (2013).

17. Sánchez-López, E. *et al.* PEGylated PLGA nanospheres optimized by design of experiments for ocular administration of dexibuprofen– in vitro, ex vivo and in vivo characterization. *Colloids Surfaces B Biointerfaces* **145,** 241–250 (2016).

18. Vega, E., Egea, M. ., Valls, O., Espina, M. & Garcai, M. . Flurbiprofen loaded biodegradable nanoparticles for ophtalmic administration. **95,** 2393–2405 (2006).

19. Abrego, G. *et al.* Design of nanosuspensions and freeze-dried PLGA nanoparticles as a novel approach for ophthalmic delivery of pranoprofen. *J. Pharm. Sci.* **103,** 3153–64 (2014).

20. Levy, M. Y. & Benita, S. Drug release from submicronized o/w emulsion: a new in vitro kinetic evaluation model. *Int. J. Pharm.* **66,** 29–37 (1990).

21. Bonakdar, M., Wasson, E. M., Lee, Y. W. & Davalos, R. V. Electroporation of Brain Endothelial Cells on Chip toward Permeabilizing the Blood-Brain Barrier. *Biophys. J.* **110,** 503–513 (2016).

22. Andreani, T. *et al.* Surface engineering of silica nanoparticles for oral insulin delivery: characterization and cell toxicity studies. *Colloids Surf. B. Biointerfaces* **123,** 916–23 (2014).

23. Fangueiro, J. F. *et al.* Design of cationic lipid nanoparticles for ocular delivery: Development, characterization and cytotoxicity. *Int. J. Pharm.* **461,** 64–73 (2014).

24. Cecchelli, R. *et al.* Modelling of the blood-brain barrier in drug discovery and development. *Nat. Rev. Drug Discov.* **6,** 650–661 (2007).

25. Burek, M., Salvador, E. & Förster, C. Y. *Concepts and models for Drug Permeability Studies*. *Woodhead publishing* (2016). doi:10.1016/B978-0-08-100094-6.00019-5

26. Vasconcelos, A. *et al.* Conjugation of cell-penetrating peptides with poly(lactic-co-glycolic acid)-polyethylene glycol nanoparticles improves ocular drug delivery. *Int. J. Nanomedicine* **10,** 609–631 (2015).

27. Zhou, Z., Badkas, A., Stevenson, M., Lee, J. Y. & Leung, Y. K. Herceptin conjugated PLGA-PHis-PEG pH sensitive nanoparticles for targeted and controlled drug delivery. *Int. J. Pharm.* **487,** 81–90 (2015).

28. Minkeviciene, R., Banerjee, P. & Tanila, H. Memantine Improves Spatial Learning in a Transgenic Mouse Model of Alzheimer's Disease. *J. Pharmacol. Exp. Ther.* **311,** 677–682 (2004).

29. Bonabello, a *et al.* Dexibuprofen (S(+)-isomer ibuprofen) reduces gastric damage and improves analgesic and anti inflammatory effects in rodents. *Anesth. Analg.* **97,** 402–408 (2003).

30. Pedrós, I. *et al.* Early alterations in energy metabolism in the hippocampus of APPswe/PS1dE9 mouse model of Alzheimer's disease. *Biochim. Biophys. Acta - Mol. Basis Dis.* **1842,** 1556–1566 (2014).

31. Chattopadhyay, M., Kodela, R., Duvalsaint, P. L. & Kashfi, K. Gastrointestinal safety , chemotherapeutic potential , and classic pharmacological profile of NOSH-naproxen (AVT-219) a dual NO- and H 2 S-releasing hybrid. 1–16 (2016). doi:10.1002/prp2.224

32. Best, R., Lewis, D. a & Nasser, N. The anti-ulcerogenic activity of the unripe plantain banana (Musa species). *Br. J. Pharmacol.* **82,** 107–116 (1984).

33. Li, Y. H., Li, J., Huang, Y., Lü, X. W. & Jin, Y. Gastroprotective effect and mechanism of amtolmetin guacyl in mice. *World J. Gastroenterol.* **10,** 3616–3620 (2004).

34. Zhang, C. *et al.* The potential use of H102 peptide-loaded dual-functional nanoparticles in the treatment of Alzheimer's disease. *J. Control. Release* **192,** 317–324 (2014).

35. Ettcheto, M. *et al.* Hypercholesterolemia and neurodegeneration. Comparison of hippocampal phenotypes in LDLr knockout and APPswe/PS1dE9 mice. *Exp. Gerontol.* **65,** 69–78 (2015).

36. Porquet, D. *et al.* Amyloid and tau pathology of familial Alzheimer's disease APP/PS1 mouse model in a senescence phenotype background (SAMP8). *Age (Omaha).* **37,** 1–17 (2015).

37. Ettcheto, M. *et al.* Evaluation of neuropathological effects of a high-fat diet in a presymptomatic Alzheimer's disease stage in APP/PS1 mice. *J. Alzheimer's Dis.* **54,** 233–251 (2016).

38. Cheng, K. K. *et al.* Highly Stabilized Curcumin Nanoparticles Tested in an In Vitro Blood–Brain Barrier Model and in Alzheimer's Disease Tg2576 Mice. *AAPS J.* **15,** 324–336 (2013).

39. Abrego, G. *et al.* Biopharmaceutical profile of pranoprofen-loaded PLGA nanoparticles containing hydrogels for ocular administration. *Eur. J. Pharm. Biopharm.* **231,** 1–10 (2015).

40. Parra, A. *et al.* Design and elaboration of freeze-dried PLGA nanoparticles for the transcorneal permeation of carprofen: Ocular anti-inflammatory applications. *Colloids Surf. B. Biointerfaces* **136,** 935–43 (2015).

41. Asadpour, E., Sadeghnia, H. R., Ghorbani, A., Sedaghat, M. & Boroushaki, M. T. Oxidative stress-mediated cytotoxicity of zirconia nanoparticles on PC12 and N2a cells. *J. Nanoparticle Res.* **18,** 14 (2016).

42. Yin, T. *et al.* Sialic acid (SA)-modified selenium nanoparticles coated with a high blood-brain barrier permeability peptide-B6 peptide for potential use in Alzheimer's disease. *Acta Biomater.* **25,** 172–183 (2015).

43. Hu, K. *et al.* Lactoferrin conjugated PEG-PLGA nanoparticles for brain delivery: Preparation, characterization and efficacy in Parkinsons disease. *Int. J. Pharm.* **415,** 273–283 (2011).

44. Semete, B. *et al.* Effects of protein binding on the biodistribution of PEGylated PLGA nanoparticles post oral administration. *Int. J. Pharm.* **424,** 115–120 (2012).

45. Griffin, B. T. *et al.* Pharmacokinetic, pharmacodynamic and biodistribution following oral administration of nanocarriers containing peptide and protein drugs. *Adv. Drug Deliv. Rev.* (2016). doi:10.1016/j.addr.2016.06.006

46. Mckee, A. C. *et al.* Ibuprofen reduces A β , hyperphosphorylated tau and memory deficits in Alzheimer mice. **7,** (2008).

47. Lee, Y.-J. *et al.* Epigallocatechin-3-gallate prevents systemic inflammation-induced memory deficiency and amyloidogenesis via its anti-neuroinflammatory properties. *J. Nutr. Biochem.* **24,** 298–310 (2013).

48. Novakova, I. *et al.* Transport rankings of non-steroidal antiinflammatory drugs across blood-brain barrier in vitro models. *PLoS One* **9,** 1–14 (2014).

49. Parepally, J. M. R., Mandula, H. & Smith, Q. R. Brain uptake of nonsteroidal anti-inflammatory drugs: Ibuprofen, flurbiprofen, and indomethacin. *Pharm. Res.* **23,** 873–881 (2006).

50. Wohlfart, S., Gelperina, S. & Kreuter, J. Transport of drugs across the blood-brain barrier by nanoparticles. *J. Control. Release* **161,** 264–73 (2012).

51. Zara, G. P. *et al.* Intravenous administration to rabbits of non-stealth and stealth doxorubicin-loaded solid lipid nanoparticles at increasing concentrations of stealth agent: pharmacokinetics and distribution of doxorubicin in brain and other tissues. *J. Drug Target.* **10,** 327–335 (2002).

52. Ortega-Martínez, S. A new perspective on the role of the CREB family of transcription factors in memory consolidation via adult hippocampal neurogenesis. *Front. Mol. Neurosci.* **8,** 1–12 (2015).

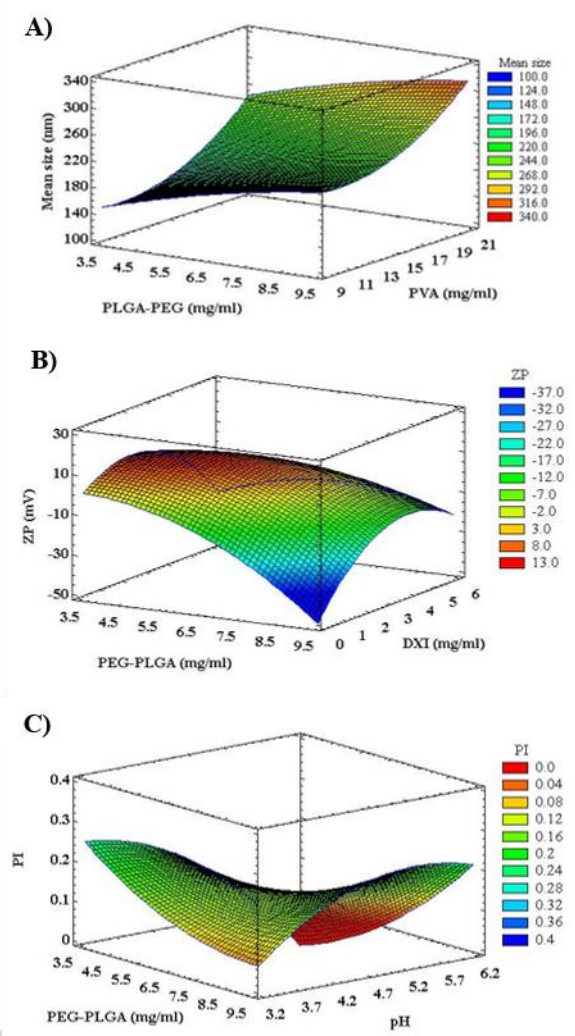

1. Surface response of DXI loaded NSs. **A)** PLGA-PEG and PVA concentration influence on NSs size, **B)** PLGA-PEG and DXI concentrations influence on NSs ZP and **C)** PLGA-PEG concentration and pH influence on NSs PI.

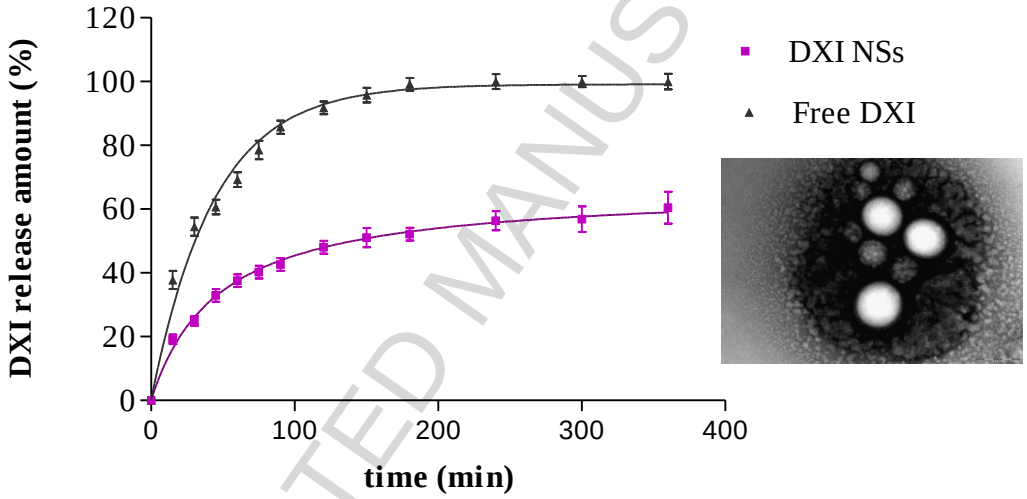

2. *In vitro* drug release of free DXI (adjusted to first order exponential kinetics) against DXI loaded NSs (adjusted to hyperbola equation) and NSs TEM.

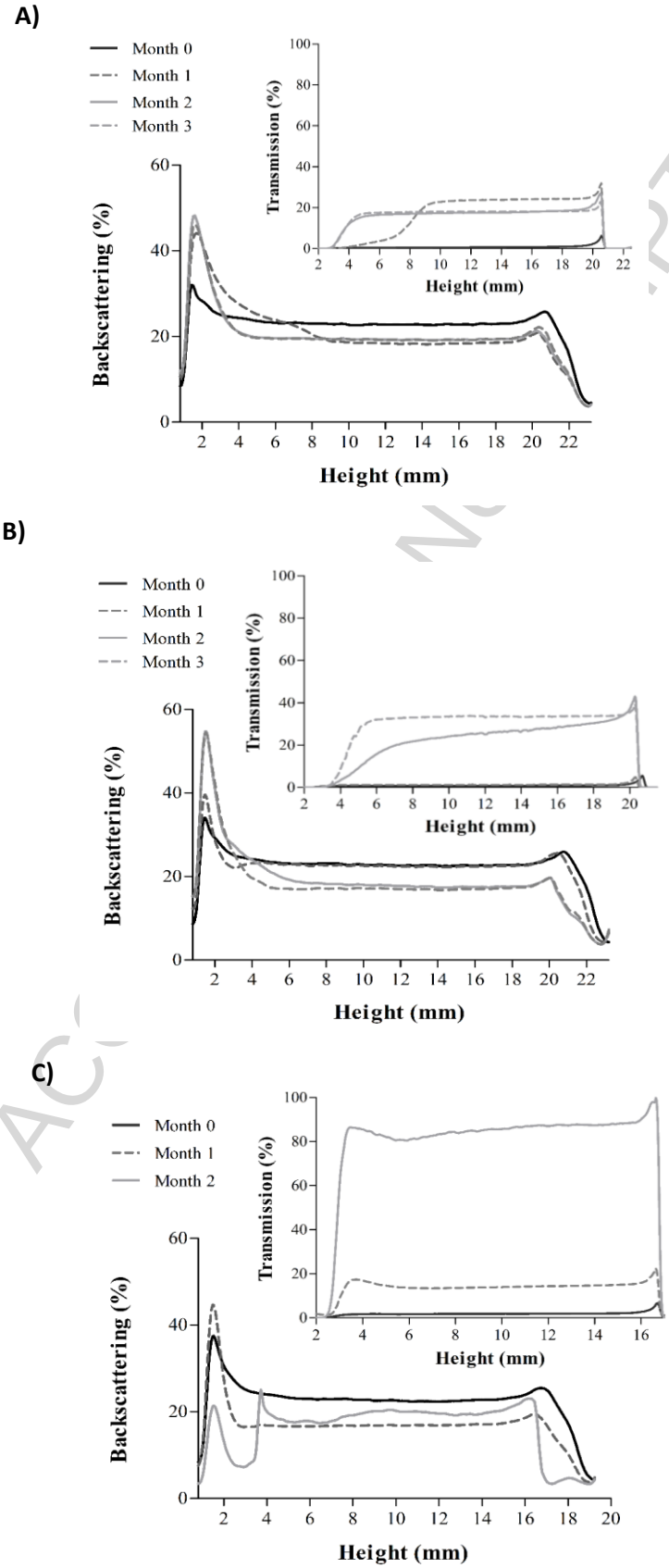

3. DXI loaded NSs backscattering and transmission profiles stored at different temperatures. **A)** 4 ^{o}C, **B)** 25 ^{o}C and **C)** 38 ^{o}C.

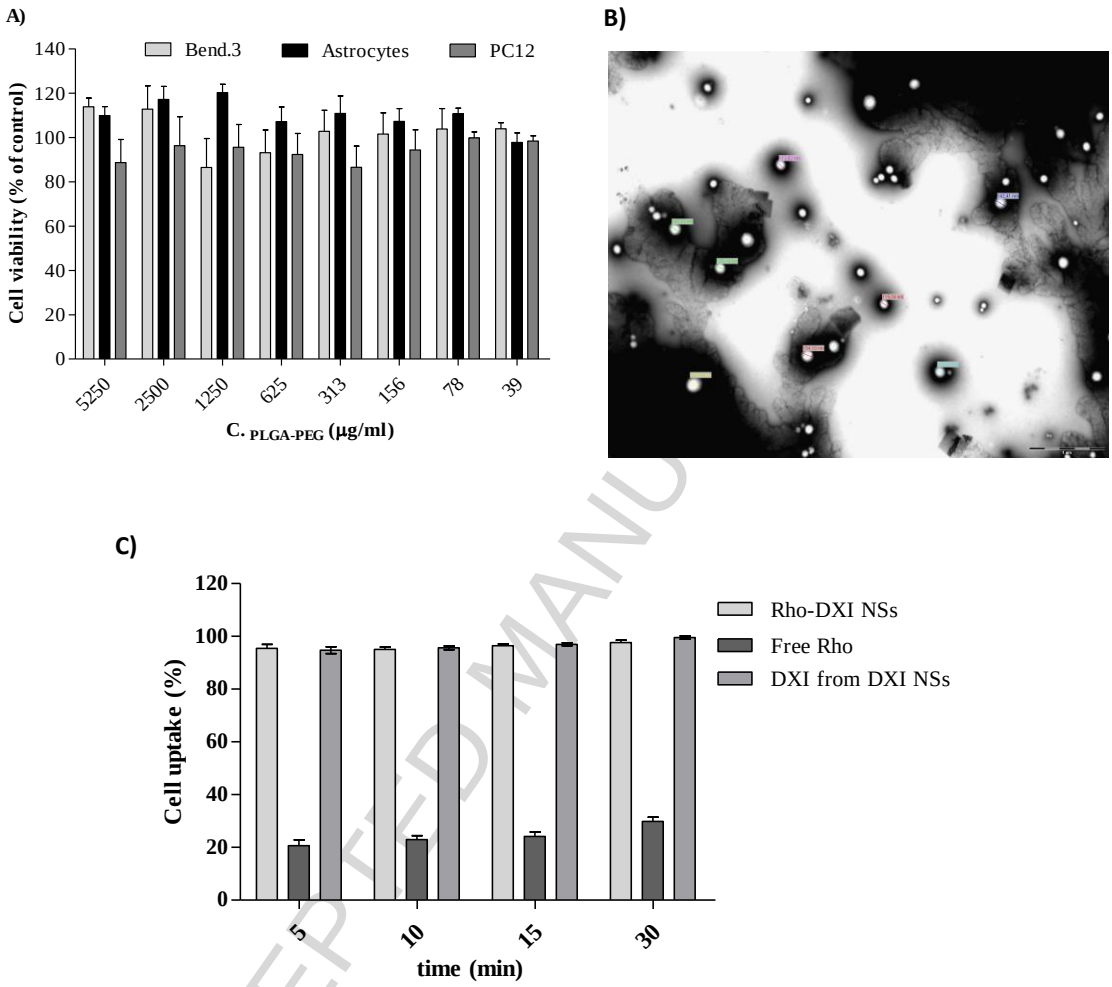

4. In vitro studies **A)** Cell viability of DXI loaded NSs with different cell lines (bEnd.3, astrocytes, PC12), **B)** TEM image of DXI loaded NSs on the basolateral media after one hour of in vitro blood-brain barrier transport assay and **C)** Cellular uptake of Rhodamine labelled NSs at different times.

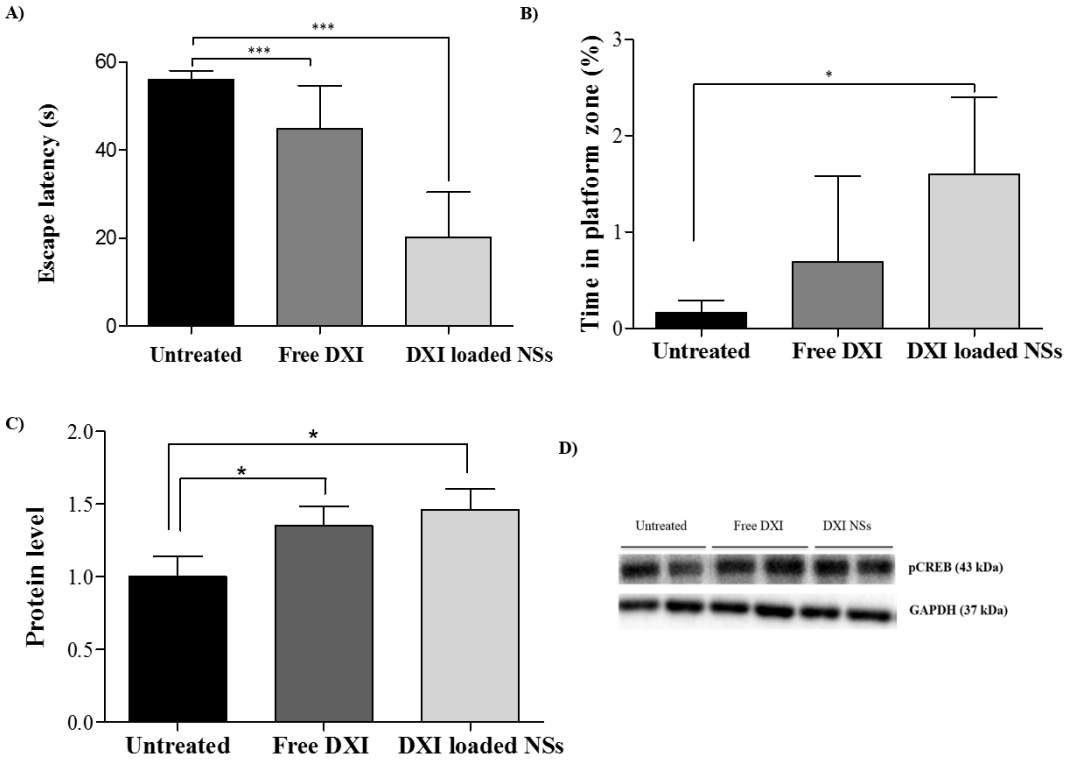

5. APP/PS1 mice results. **A)** Morris water maze escape latency on the probe trial, **B)** Morris water maze escape latency time in platform zone on the probe trial, **C)** Mean pCREB levels and **D)** Representative western blot of pCREB extracted from hippocampus.

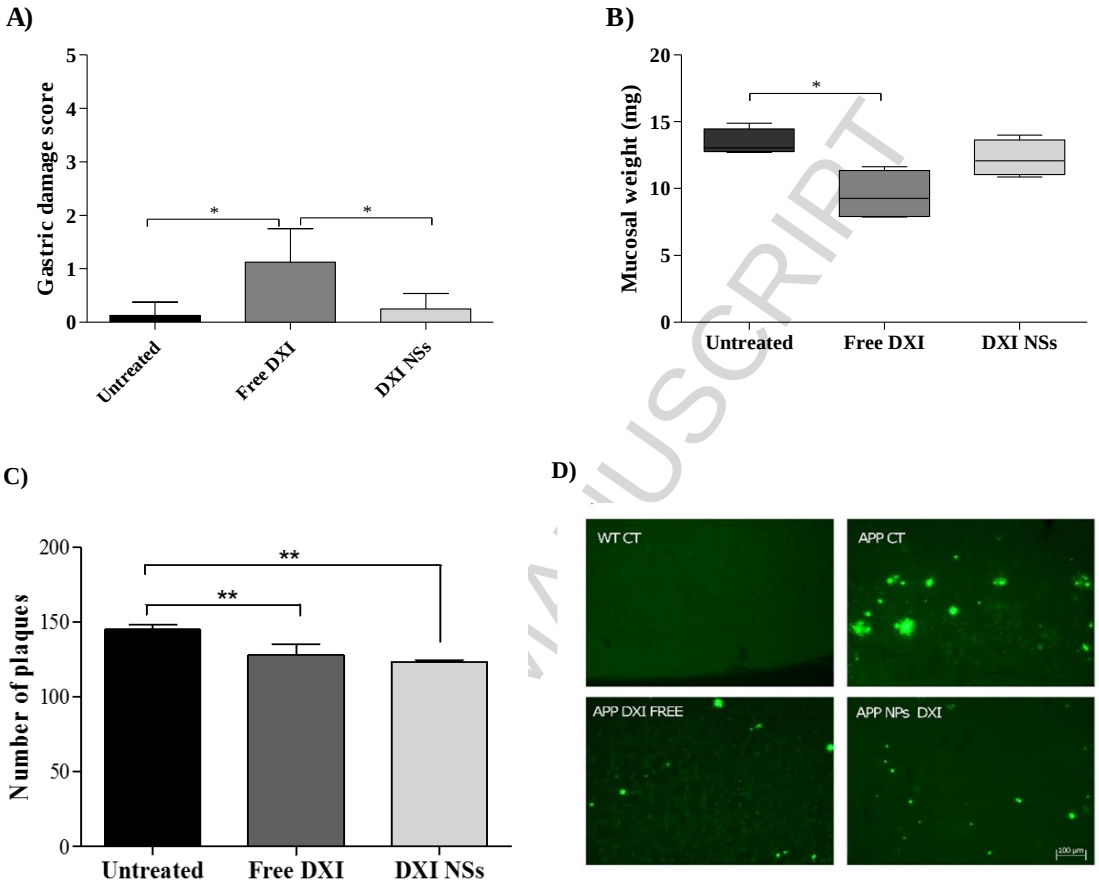

6. In vivo studies after DXI treatment. **A)** Gastric damage score, **B)** Mucosal weight after freeze-drying, **C)** Mean counting of β-amyloid plaques in brain cortex after Th-S staining and **D)** Representative microscopic images of β-amyloid plaques.

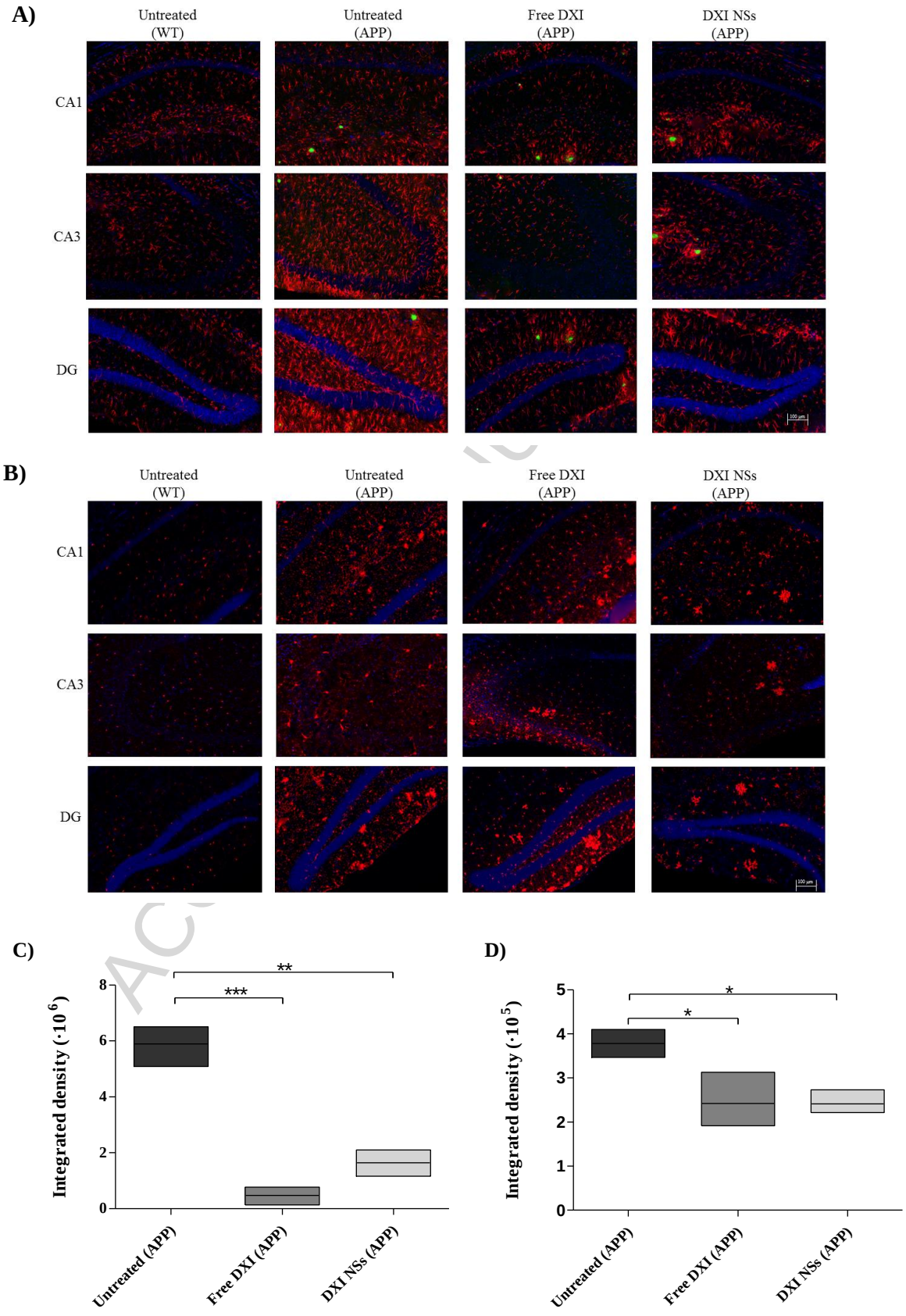

7. Detection of inflammatory markers on hippocampus subfields on APP/PS1 mice. **A)** Immunostained for GFAP, ThS and Hoetsch, **B)** Immunostained for IBA-1 and Hoestch, **C)** Quantification of GFAP and **D)** Quantification of IBA-1

Table 1. Design of experiments of DXI loaded NSs.

	c. PLGA PEG (mg/ml)		c. PVA (mg/ml)		c. DXI (mg/ml)		pH		Z_{av} (nm)	PI	ZP (mV)	EE (%)
Factorial points												
F1	1	7.5	-1	12.0	-1	1.5	-1	3.8	212.6 ± 1.0	0.166 ± 0.016	-11.1 ± 0.3	91.06
F2	1	7.5	1	18.0	-1	1.5	1	5.3	193.8 ± 1.0	0.057 ± 0.013	-12.3 ± 0.5	81.22
F3	-1	4.5	-1	12.0	1	4.5	1	5.3	170.2 ± 1.0	0.055 ± 0.010	-6.3 ± 0.7	90.81
F4	-1	4.5	1	18.0	1	4.5	1	5.3	166.4 ± 1.3	0.074 ± 0.021	-9.9 ± 0.9	99.99
F5	-1	4.5	-1	12.0	-1	1.5	1	5.3	161.6 ± 0.7	0.085 ± 0.001	-9.0 ± 0.3	88.13
F6	-1	4.5	1	18.0	1	4.5	-1	3.8	168.5 ± 1.1	0.091 ± 0.032	-8.4 ± 0.6	97.73
F7	1	7.5	-1	12.0	1	4.5	1	5.3	192.4 ± 1.0	0.052 ± 0.019	-8.3 ± 1.7	94.38
F8	1	7.5	1	18.0	1	4.5	-1	3.8	222.1 ± 29.7	0.171 ± 0.066	-3.2 ± 4.3	97.99
F9	-1	4.5	-1	12.0	1	4.5	-1	3.8	103.2 ± 96.4	0.369 ± 0.547	-0.1 ± 0.3	95.40
F10	1	7.5	1	18.0	-1	1.5	-1	3.8	249.6 ± 5.3	0.205 ± 0.018	-17.1 ± 0.6	96.47
F11	-1	4.5	1	18.0	-1	1.5	-1	3.8	260.7 ± 11.0	0.314 ± 0.012	-12.5 ± 1.1	95.36
F12	-1	4.5	1	18.0	-1	1.5	1	5.3	163.9 ± 0.6	0.060 ± 0.018	-7.4 ± 0.8	92.78
F13	1	7.5	-1	12.0	-1	1.5	1	5.3	199.4 ± 10.4	0.203 ± 0.029	-11.7 ± 0.4	87.18
F14	1	7.5	1	18.0	1	4.5	1	5.3	293.6 ± 6.7	0.235 ± 0.039	-15.1 ± 0.9	96.82
F15	-1	4.5	-1	12.0	-1	1.5	-1	3.8	185.4 ± 1.3	0.053 ± 0.015	-8.6 ± 0.8	93.16
F16	1	7.5	-1	12.0	1	4.5	-1	3.8	196.5 ± 0.9	0.068 ± 0.006	-5.9 ± 0.5	93.04
Axial points												
F17	0	6	0	15.0	0	3.0	-1.68	3.2	181.3 ± 1.1	0.069 ± 0.027	-8.1 ± 3.7	97.94
F18	0	6	-1.68	10.0	0	3.0	0	4.5	177.8 ± 1.1	0.060 ± 0.009	-12.4 ± 0.5	95.23
F19	-1.68	3.5	0	15.0	0	3.0	0	4.5	196.9 ± 2.7	0.207 ± 0.014	-10.3 ± 0.5	94.35
F20	0	6	0	15.0	0	3.0	0	4.5	204.7 ± 4.1	0.151 ± 0.027	-9.4 ± 0.7	88.69
F21	0	6	1.68	20.0	0	3.0	0	4.5	310.7 ± 21.8	0.197 ± 0.046	-12.9 ± 0.5	96.42
F22	0	6	0	15.0	-1.68	0.5	0	4.5	214.7 ± 9.47	0.212 ± 0.052	-16.2 ± 0.3	81.75
F23	0	6	0	15.0	1.68	5.5	0	4.5	227.8 ± 17.7	0.224 ± 0.014	-11.7 ± 0.1	96.77
F24	1.68	8.5	0	15.0	0	3.0	0	4.5	230.4 ± 20.2	0.191 ± 0.032	-19.0 ± 0.6	99.20
F25	0	6	0	15.0	0	3.0	1.68	5.8	180.1 ± 4.7	0.073 ± 0.039	-11.9 ± 0.5	94.45
Central points												
F26	0	6	0	15.0	0	3.0	0	4.5	204.7 ± 0.4	0.151 ± 0.008	-9.4 ± 0.3	88.69
F27	0	6	0	15.0	0	3.0	0	4.5	172.6 ± 1.0	0.083 ±0.025	-8.8 ± 0.6	99.19

Graphical Abstract

Dexibuprofen loaded PEGylated nanospheres were developed and administered *in vivo* for Alzheimer's disease prevention. These nanosystems contribute to Dexibuprofen delivery into the brain.

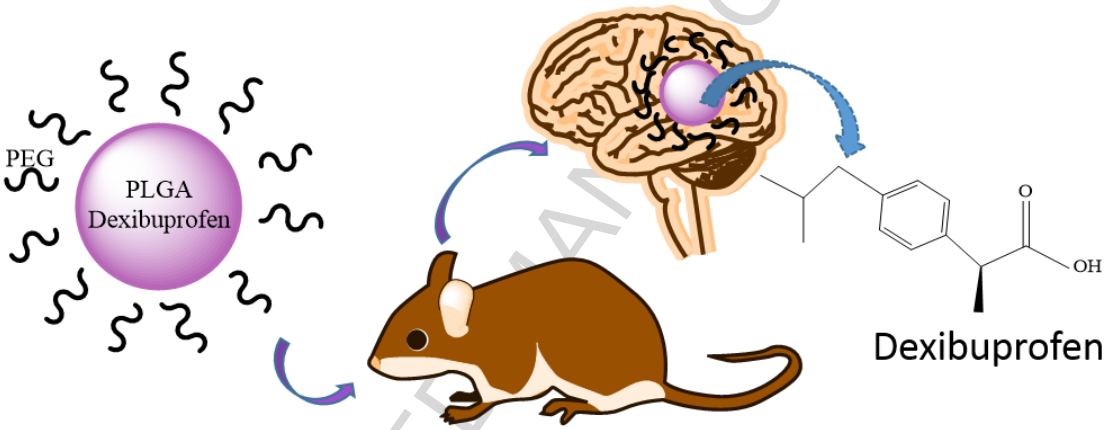

Highlights

- Factorial design has been proven to be useful to optimize Dexibuprofen loaded nanospheres
- The *in vitro* release profile of Dexibuprofen nanospheres against free drug showed that the drug loaded NSs present a sustained release, slower than the free drug
- Developed nanosystems increase drug transport across the blood-brain barrier
- Gastric damage produced by free Dexibuprofen is reduced by drug loading to biodegradable NSs
- Dexibuprofen NSs decrease memory impairment associated with Alzheimer's more efficiently than the free drug.